Neurobiology of Disease

Loss of MeCP2 From Forebrain Excitatory Neurons Leads to Cortical Hyperexcitation and Seizures

Wen Zhang, Matthew Peterson, Barbara Beyer, Wayne N. Frankel, and Zhong-wei Zhang
The Jackson Laboratory, Bar Harbor, Maine 04609

Mutations of *MECP2* cause Rett syndrome (RTT), a neurodevelopmental disorder leading to loss of motor and cognitive functions, impaired social interactions, and seizure at young ages. Defects of neuronal circuit development and function are thought to be responsible for the symptoms of RTT. The majority of RTT patients show recurrent seizures, indicating that neuronal hyperexcitation is a common feature of RTT. However, mechanisms underlying hyperexcitation in RTT are poorly understood. Here we show that deletion of *Mecp2* from cortical excitatory neurons but not forebrain inhibitory neurons in the mouse leads to spontaneous seizures. Selective deletion of *Mecp2* from excitatory but not inhibitory neurons in the forebrain reduces GABAergic transmission in layer 5 pyramidal neurons in the prefrontal and somatosensory cortices. Loss of MeCP2 from cortical excitatory neurons reduces the number of GABAergic synapses in the cortex, and enhances the excitability of layer 5 pyramidal neurons. Using single-cell deletion of *Mecp2* in layer 2/3 pyramidal neurons, we show that GABAergic transmission is reduced in neurons without MeCP2, but is normal in neighboring neurons with MeCP2. Together, these results suggest that MeCP2 in cortical excitatory neurons plays a critical role in the regulation of GABAergic transmission and cortical excitability.

Key words: **GABA; hyperexcitation; neocortex; pyramidal neuron; Rett syndrome; seizure**

Introduction

Loss-of-function mutations of X-linked *MECP2* (methyl-CpG binding protein 2) cause the pervasive Rett syndrome (RTT; Chahrour and Zoghbi, 2007). RTT patients show progressive loss of motor and cognitive functions, impaired social interactions, anxiety, and seizure at young ages. Studies using mouse models of RTT have demonstrated that loss of MeCP2 from the brain is responsible for the neurological symptoms of RTT (Chen et al., 2001). However, the underlying mechanisms are largely unknown. Despite a reduction in brain size in RTT patients, there is no obvious change in the number of neurons or general pattern of brain organization (Armstrong, 2005); similar results have been found in mouse models of RTT (Chen et al., 2001; Guy et al., 2001; Shahbazian et al., 2002). It has been hypothesized that defects of neuronal circuit development and function are a major mechanism of RTT (Chahrour and Zoghbi, 2007). This hypothesis is supported by several studies demonstrating synaptic defects in MeCP2-deficient mice during development and in adulthood. Excitatory synaptic transmission is reduced in hippocampal cultures from *Mecp2* knock-out mice (Nelson et al., 2006; Chao et al., 2007), but increased in those from mice overexpressing *Mecp2* (Chao et al., 2007; Na et al., 2012). Long-term plasticity of excitatory synapses is also impaired in hippocampal slices of MeCP2-deficient mice (Asaka et al., 2006; Moretti et al., 2006; Guy et al., 2007). Changes of inhibitory transmission have been reported in the cortex, brainstem, hippocampus, and thalamus of *Mecp2* knock-out mice (Dani et al., 2005; Medrihan et al., 2008; Zhang et al., 2008, 2010).

Clinical studies have shown that 70–80% of RTT patients have recurrent seizures, with the onset typically between 2 and 5 years of age (Jian et al., 2007; Nissenkorn et al., 2010; Pintaudi et al., 2010; Cardoza et al., 2011). Both partial and generalized seizures are common, and electroencephalographic (EEG) data reveal focal and generalized epileptic discharges in RTT patients (Nissenkorn et al., 2010; Vignoli et al., 2010). Furthermore, abnormal EEG activity in RTT patients is negatively correlated with their cognitive and communication abilities (Vignoli et al., 2010). These studies indicate that in addition to seizures, cognitive and behavioral disabilities in RTT may be caused by a hyperactivity of the neocortex and associated brain regions. How MeCP2 deficiency leads to cortical hyperexcitation is poorly understood. *Mecp2* knock-out mice display seizures and hyperexcitability discharges, indicating that as in human, deficiency of MeCP2 causes network hyperexcitation in the brain (Chao et al., 2010; D'Cruz et al., 2010; Calfa et al., 2011). A concern with this model, however, is that there are widespread neuronal defects in the brain of *Mecp2* knock-out mice (Wang et al., 2006; Medrihan et al., 2008; Taneja et al., 2009; Zhang et al., 2010; Noutel et al., 2011), therefore any changes observed in the cortex may be caused by defects in other brain regions. Furthermore, MeCP2 may have distinct roles in different types of cells. To address these issues, we examined mice with forebrain-restricted and cell-type-specific deletion of *Mecp2*.

Received Oct. 17, 2012; revised Jan. 11, 2014; accepted Jan. 15, 2014.

Author contributions: Z.-w.Z. designed research; W.Z., M.P., B.B., and Z.-w.Z. performed research; W.Z., M.P., W.N.F., and Z.-w.Z. analyzed data; W.Z. and Z.-w.Z. wrote the paper.

This work was supported by NIH Grants NS082658 (Z.-w.Z.), NS064013 (Z.-w.Z.), and NS031348 (W.N.F.). We thank Da-Ting Lin and Kevin Seburn for comments on the paper, and Verity Letts and Hong Liu for expert assistance.

Correspondence should be addressed to Dr Zhong-wei Zhang, The Jackson Laboratory, 600 Main Street, Bar Harbor, ME 04609. E-mail: zhongwei.zhang@jax.org.

W. Zhang's present address: National Institute on Drug Abuse Intramural Research Program, Baltimore, MD 21224.

DOI:10.1523/JNEUROSCI.4900-12.2014
 0270-6474/14/342754-10$15.00/0

Materials and Methods

Mice. Mice carrying the *Mecp2* conditional allele (B6.129S4-*Mecp2*^{tm1Jae}/Mmucd; *Mecp2*^{F}; Chen et al., 2001) were obtained from the Mutant Mouse Regional Center (MMRRC; stock No. 011918-UCD), and backcrossed to C57BL/6J (B6) for >10 generations. Cre driver strains *Emx1*-Cre (B6.129S2-*Emx1*$^{tm1(cre)Krj}$/J; Gorski et al., 2002), *Dlx5/6*-Cre (Tg(*Dlx6a*-Cre)1Mekk/J; Monory et al., 2006), and Rosa-tdTomato reporter (Ai14; Madisen et al., 2010) were obtained from JAX (stock No. 5628, 8199, and 7914, respectively). The *Emx1*-Cre strain was on a B6 background; the *Dlx5/6-Cre* strain was backcrossed to B6 for eight generations. The serotonin transporter (SERT) Cre strain (Tg(*Slc6a4*-Cre)ET124Gsat, or SERT-Cre), generated by GENSAT (Gong et al., 2007), was obtained from the MMRRC (stock No. 017261-UCD). Originally, on a mixed FVB/B6/129/Swiss background, this strain was backcrossed to B6 for six generations before the experiments.

Genotypes were determined by PCR using tail DNA. For the *Mecp2*^{F} strain, the primers were 5′-CTAGGTAAGAGCTCTTGTTGA-3′ and 5′-CACCACAGAAGTACTATGATC-3′, which gave products of 280 and 180 bp for the mutant and wild-type alleles, respectively. Cre driver strains were genotyped using primers 5′-GCATTACCGGTCGATGCA ACGAGTGATGAG-3′ and 5′-GAGTGAACGAACCTGGTCGAAATCA GTGCG-3′, which amplify a 410 bp fragment.

All procedures are in accordance with the NIH *Guide for the Care and Use of Laboratory Animals*, and have been approved by The Jackson Laboratory Animal Care and Use Committee.

EEG recording. EEG was recorded from male mice of 6–8 weeks of age using procedures that we described previously (Beyer et al., 2008). Briefly, mice were anesthetized with tribromoethanol (400 mg/kg i.p.). Four small holes were drilled on the skull (1 mm anterior and 2 mm posterior to the bregma, 2 mm lateral to the midline). One Teflon-coated silver wire was inserted into each hole and placed between the dura and skull. The wires were soldered onto a microconnector that was fixed on the skull using dental cement. The mice were given a 48 h recovery period before recordings were made. EEG was recorded for a 2 h period on each of the following 2 d (Stellate Harmonie, Stellate Systems).

Slice preparation. Male mice aged P17–P20 and P42–P50 were anesthetized with tribromo-ethanol and decapitated. Coronal sections 300 μm thick were prepared with a vibratome (Leica VT1200). Slices were kept in artificial CSF (ACSF) containing the following (in mM): 124 NaCl, 3.0 KCl, 1.5 $CaCl_2$, 1.3 $MgCl_2$, 1.0 NaH_2PO_4, 26 $NaHCO_3$, and 20 glucose, saturated with 95% O_2 and 5% CO_2 at room temperature (21–23°C).

Patch-clamp recording. Layer 5 pyramidal neurons in the medial prefrontal cortex (mPFC) and the barrel cortex (S1) were recorded using methods that we described previously (Zhang, 2004). A slice was transferred to a submersion type chamber where it was continuously perfused with ACSF saturated with 95% O_2 and 5% CO_2 at 32–33°C. The slice was first viewed with a 4× objective, and the mPFC was identified as the area between the forceps minor corpus callosum and the midline. The S1 barrel cortex was identified based on characteristic of the layer 4. Pyramidal neurons were identified with a 40× objective and Nomarski optics. For IPSC recording, the pipette solution contained the following (in mM): 120 CsCl, 20 TEA-Cl, 4 ATP-Mg, 0.3 GTP, 0.5 EGTA, 10 HEPES, and 4.0 QX-314 (pH 7.2, 270–280 mOsm with sucrose). For EPSC recording, the pipette solution contained the following (in mM): 110 Cs methylsulfate, 15 CsCl, 20 TEA-Cl, 4 ATP-Mg, 0.3 GTP, 0.5 EGTA, 10 HEPES, and 4.0 QX-314 (pH 7.2, 270–280 mOsm with sucrose). Electrodes had resistances between 2 and 4 MΩ. Whole-cell recordings were made at the soma with a multiclamp 700B amplifier (Molecular Devices). The series resistance, usually between 8 and 14 MΩ, was not compensated in voltage-clamp experiments. Data were discarded when series resistance was >16 MΩ. In some experiments, bipolar electrodes made of insulated microwires (30 μm outside diameter) were placed in layer 5 to apply stimuli (100 μs, 20–300 μA). Experiments were conducted using AxoGraph X (AxoGraph Scientific). Data were filtered at 4 kHz and digitized at 20 kHz. Spontaneous synaptic events were analyzed using the event detection function of AxoGraph.

For current-clamp recording, the pipette solution contained the following (in mM): 120 K-gluconate, 10 KCl, 4 ATP-Mg, 0.3 GTP, 10 HEPES, and 0.5 EGTA (pH 7.2, 270–280 mOsm with sucrose). Series resistance was fully compensated using the bridge circuit of the amplifier MultiClamp 700B. Intrinsic properties were analyzed using methods that we described previously (Zhang, 2004; Zhang and Arsenault, 2005). Briefly, resting potentials of neurons were measured within 20 s of establishing whole-cell configuration. Input resistance was estimated from voltage responses to 400 ms current pulses at −100 pA. Action potentials were evoked using positive current pulses. Action potential threshold was estimated as the point when the slope of rising membrane potential exceeds 50 mV/ms, and for each cell, measurements of 4–6 action potentials were averaged.

Immunostaining. Mice were anesthetized with tribromoethanol, perfused with 4% paraformaldehyde in 0.1 M PBS, and postfixed overnight.

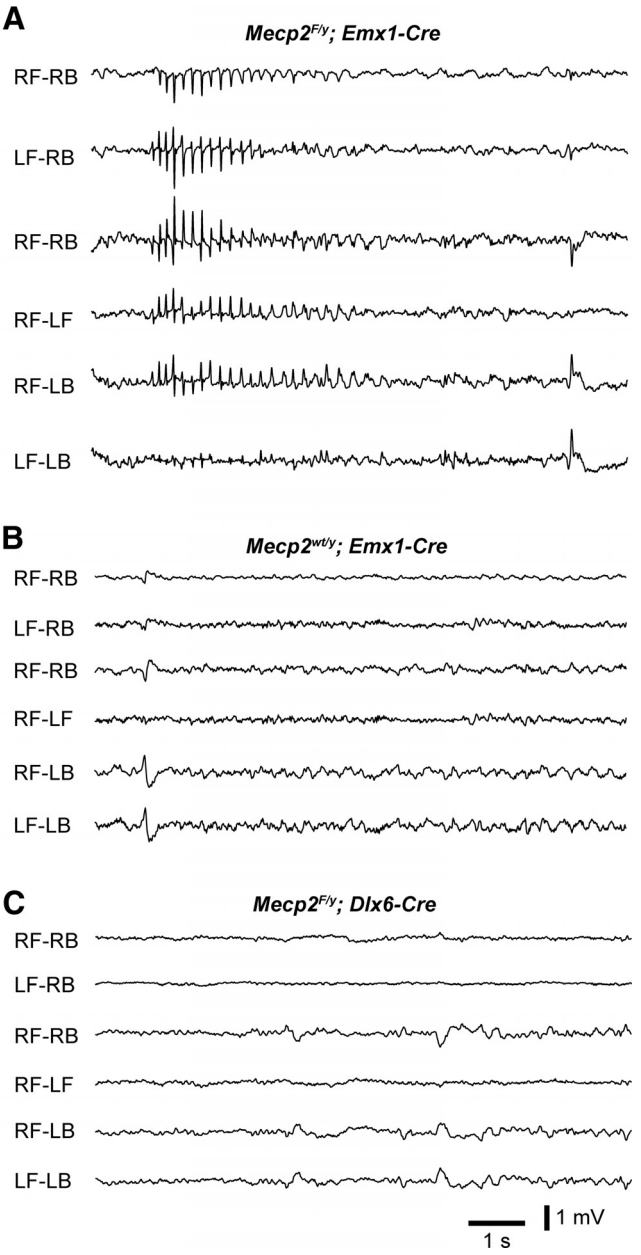

Figure 1. Conditional deletion of *Mecp2* with *Emx1*-Cre leads to spike-wave discharges. ***A***, Seizure activity in an *Emx1-Mecp2* mutant mouse at 7 weeks of age. EEG was recorded from a wake *Emx1-Mecp2* mouse using four electrodes placed over the right frontal (RF), left frontal (LF), right back (RB), and left back (LB) surface of the neocortex. Each trace is the differential between signals recorded from two of the electrodes. ***B***, EEG recording from a control mouse (*Mecp2*$^{wt/y}$; *Emx1*-Cre) at 7 weeks of age. ***C***, EEG recording from a *Dlx6a-Mecp2* mutant mouse at 7 weeks of age.

Coronal sections of 60 μm thick were cut on a vibratome. Sections containing mPFC were incubated with 1% BSA, 0.3% Triton X-100, and 3% normal goat serum for 2 h at room temperature, then incubated with polyclonal antibodies of vesicular GABA transporter (VGAT; 1:2000, Synaptic Systems), monoclonal anti-NeuN (1:1000, Millipore), polyclonal RFP (1:2000, Rockland), polyclonal anti-GABA (1:4000, Immunostar), or monoclonal anti-MeCP2 (1:1000, Cell Signaling Technology) for 48 h at 4°C. After wash, sections were incubated with goat AlexaFluor-conjugated secondary antibodies (1:500, Invitrogen) for 2 h at room temperature. Sections were mounted in DPX medium (Sigma-Aldrich).

Confocal images were taken on a Leica SP5 microscope. For VGAT straining, confocal stacks were taken with a 63× objective (NA 1.3) and 4× optical zoom. The pixel size was 60.3 nm. The *z*-step size was 130 nm, and each stack had 15 steps. Three stacks were obtained from each mouse, and the same laser and microscope setting was used for control and mutant samples. Confocal stacks were analyzed blind to the genotypes using the spot analysis tool of Imaris (Bitplane). The detection threshold was set using images that showed the strongest VGAT staining; the same threshold was applied to all stacks from control and mutant mice of the same experiment. The minimal spot size was set at 0.4 μm (X or Y). VGAT puncta was detected for the volume of the stack (6425 μm^3 without shrinkage correction), and the results were expressed as the number of VGAT puncta per 1000 μm^3 of tissue.

Statistics. Statistics was performed using IgorPro (WaveMetrics), InStat (GraphPad), and JMP (SAS). Throughout, means are given as ±SEM. Unless specified otherwise, means were compared using Mann–Whitney test or one-way ANOVA. Distributions of synaptic events were compared with Kolmogorov–Smirnov test (K–S test).

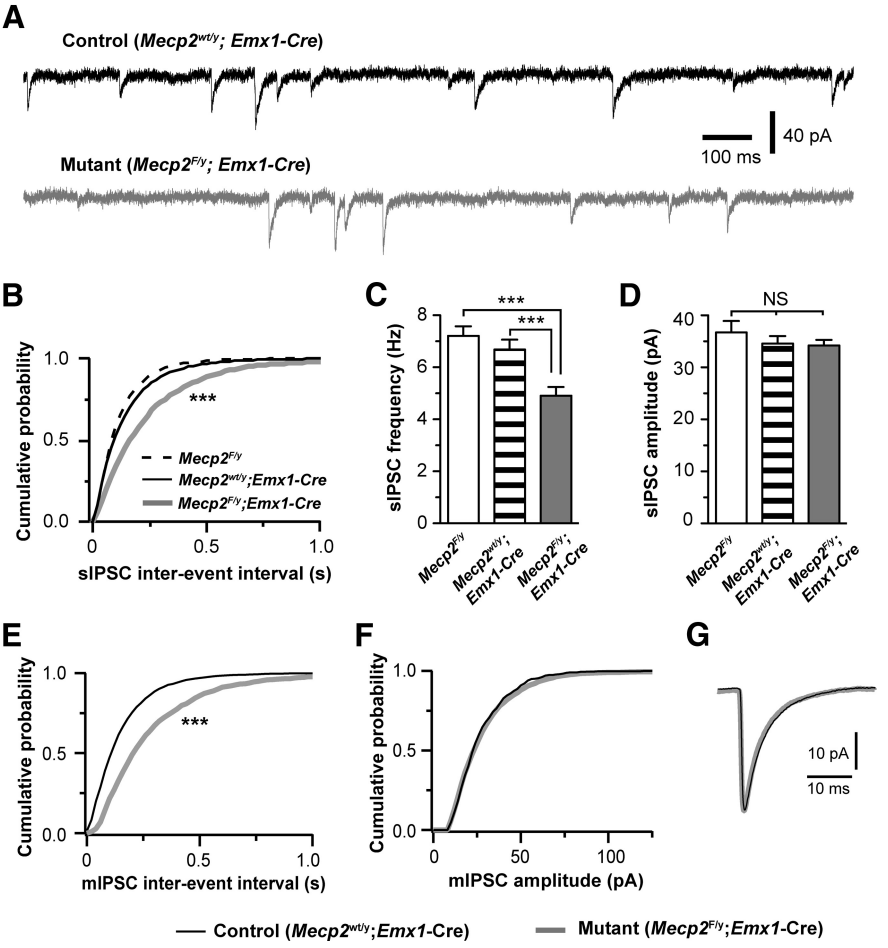

Figure 2. Deletion of *Mecp2* with *Emx1*-Cre caused reduction in the frequency of sIPSCs and mIPSCs in layer 5 pyramidal neurons in the mPFC at P17–P20. ***A***, sIPSCs recorded from a control (top trace) and mutant (bottom trace) neurons at P18. ***B***, Distributions of sIPSC intervals for mutant neurons (*Mecp2*$^{F/y}$; *Emx1*-Cre, line in gray, $n = 25$ from 4 mice) and control neurons (*Mecp2*$^{F/y}$, dashed line, $n = 15$ from 2 mice; *Mecp2*$^{wt/y}$; *Emx1*-Cre, line in black, $n = 27$ from 4 mice). For each group, the distribution was established using 200 consecutive events from each of the recorded cells; $p = 0.0007$, K–S test. ***C***, The mean frequency of sIPSCs for the three groups (4.9 ± 0.3 Hz for *Mecp2*$^{F/y}$;*Emx1*-Cre; 6.7 ± 0.4 Hz for *Mecp2*$^{wt/y}$;*Emx1*-Cre; 7.1 ± 0.3 Hz for *Mecp2*$^{F/y}$; ***$p <$ 0.001). ***D***, The mean peak amplitude of sIPSCs for the three groups (34.2 ± 1.1 pA for *Mecp2*$^{F/y}$;*Emx1-Cre*; 34.6 ± 1.4 pA for *Mecp2*$^{wt/y}$;*Emx1-Cre*; and 36.7 ± 2.2 pA for *Mecp2*$^{F/y}$; $p > 0.3$). The mean decay constant of sIPSC was 5.6 ± 0.3 ms for mutant neurons (*Mecp2*$^{F/y}$; *Emx1*-Cre), 5.5 ± 0.2 ms for *Mecp2*$^{F/y}$ control, and 5.8 ± 0.2 ms for *Mecp2*$^{wt/y}$; *Emx1*-Cre control ($p = 0.53$, one-way ANOVA). ***E***, Distributions of mIPSC intervals for mutant neurons (*Mecp2*$^{F/y}$; *Emx1*-Cre, gray) and control neurons (*Mecp2*$^{wt/y}$; *Emx1*-Cre, black). $p =$ 0.0003, K–S test. The mean frequency of mIPSC was 4.5 ± 0.2 Hz ($n = 22$ from 3 mice) for mutant neurons, and 6.4 ± 0.5 Hz ($n = 24$ from 3 mice) for control neurons ($p = 0.001$). ***F***, Distributions of mIPSC amplitude for mutant neurons (*Mecp2*$^{F/y}$; *Emx1*-Cre, gray) and control neurons (*Mecp2*$^{wt/y}$; *Emx1*-Cre, black). The mean peak amplitude of mIPSC was 28.1 ± 1.2 pA for mutant neurons, and 28.5 ± 1.3 pA for control neurons ($p = 0.68$). ***G***, Averaged mIPSCs for mutant and control neurons. The mean decay constant of mIPSC was 6.1 ± 0.2 ms for mutant neurons, and 5.7 ± 0.2 ms for control neurons ($p = 0.08$).

Results

Spontaneous seizures in mice lacking MeCP2 from the forebrain

EEG recordings revealed cortical hyperexcitation and seizures in MeCP2-deficient mice (Shahbazian et al., 2002; Zhang et al., 2008). This increase of cortical discharges may be caused by the loss of MeCP2 from excitatory or inhibitory neurons, or glia in the cortex and subcortical regions. To determine the cellular origin of cortical hyperexcitation in *Mecp2* mutant mice, we performed EEG recordings from mice lacking MeCP2 from specific cell types in the forebrain. The *Emx1*-Cre driver (Gorski et al., 2002) and a conditional *Mecp2* strain (Chen et al., 2001) were used to delete *Mecp2* from excitatory neurons and glia but not inhibitory neurons in the neocortex and hippocampus. A total of five *Emx1-Mecp2* (*Mecp2*$^{F/y}$; *Emx1*-Cre) mutant mice were recorded between 6 and 8 weeks of age. We found that all *Emx1-Mecp2* mutant mice showed absence seizures as characterized by spike-wave discharges in animals that were awake (Fig. 1*A*). Spike-wave discharges occurred at 36 ± 7 episodes/h ($n = 5$ mice), and the mean duration of episode was 1.3 ± 0.1 s. In contrast, all four control mice that we recorded did not show any spike-wave discharges (Fig. 1*B*). We also recorded five mice lacking MeCP2 from inhibitory neurons in the forebrain using the *Dlx6a*-Cre driver (Monory et al., 2006). None of the *Dlx6a-Mecp2* (*Mecp2*$^{F/y}$; *Dlx6a*-Cre) mutant mice showed any spike-wave discharges (Fig. 1*C*). These results indicate that loss of MeCP2 from excitatory neurons and glia in the forebrain is sufficient to cause hyperexcitation and seizures.

GABAergic transmission is reduced in the cortex of mice lacking MeCP2 from the forebrain excitatory neurons

The seizure phenotype observed in *Emx1-Mecp2* mice suggests that the balance of excitation and inhibition (E/I balance) is disrupted in these mice. In addition to seizures, shift in E/I balance is also implicated in other RTT symptoms, such as cognitive defects, anxiety, and impaired social behaviors (Yizhar et al., 2011).

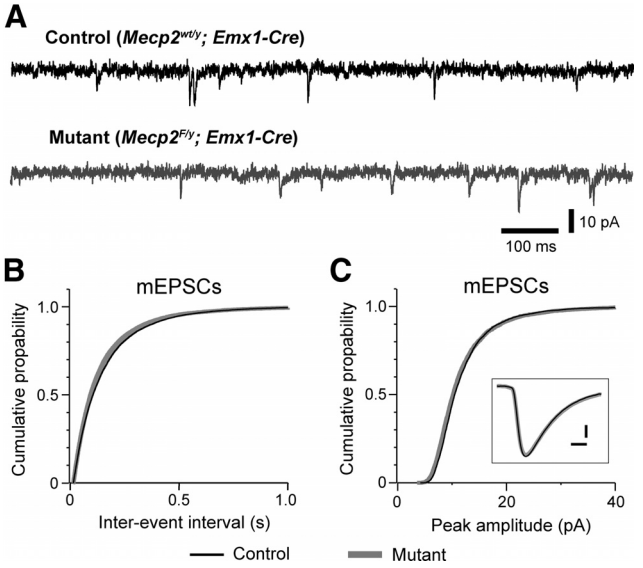

Figure 3. Deletion of *Mecp2* with *Emx1*-Cre had no effect on excitatory transmission in the prefrontal cortex. ***A***, mEPSCs recorded from a control (top trace, black) and mutant (bottom trace, gray) layer 5 pyramidal neurons in mPFC at P18 in presence of TTX (0.3 μM) and picrotoxin (100 μM). ***B***, Distributions of mEPSC intervals for mutant (black) and mutant (gray) neurons. The mean frequency was 6.3 $\pm$ 0.6 Hz for control neurons ($n = 24$ from 3 mice) and 6.4 $\pm$ 0.6 Hz for mutant neurons ($n = 21$ from 3 mice; $p = 0.71$). ***C***, Distributions of mEPSC peak amplitude for control (black) and mutant (gray) neurons. The mean peak amplitude was 11.8 $\pm$ 0.4 pA for control and 12.0 $\pm$ 0.3 pA for mutant neurons ($p = 0.99$). Inset, Averaged mEPSCs for control (black) and mutant (gray) neurons. Scale bars, 2 pA and 2 ms. The mean decay constant of mEPSCs was 3.7 $\pm$ 0.1 ms for control and 3.8 $\pm$ 0.1 ms for mutant neurons ($p = 0.89$).

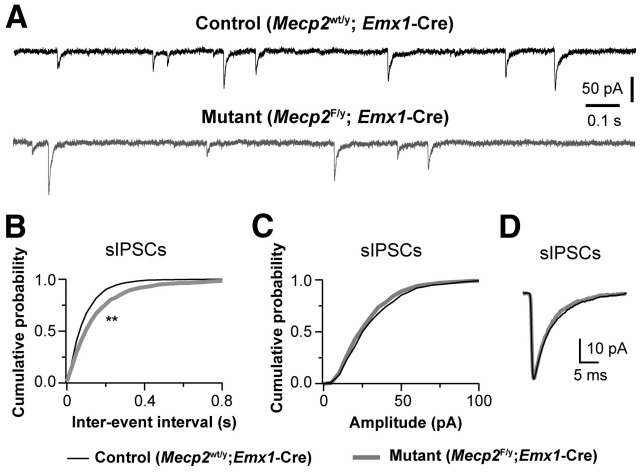

Figure 4. Deletion of *Mecp2* with *Emx1*-Cre reduced GABAergic transmission in the somatosensory cortex. ***A***, sIPSCs recorded from a control (top trace, black) and mutant (bottom trace, gray) layer 5 pyramidal neurons in S1 at P18. ***B***, Distributions of sIPSC intervals for mutant neurons (*Mecp2*$^{F/y}$; *Emx1*-Cre, gray) and control neurons (*Mecp2*$^{wt/y}$; *Emx1*-Cre, black); $^{**}p <$ 0.001, K–S test. The mean frequency of sIPSCs for control (8.7 $\pm$ 0.4 Hz, $n = 17$ cells from 3 mice) and mutant neurons (6.5 $\pm$ 0.6 Hz, $n = 19$ cells from 3 mice; $^{**}p = 0.004$). ***C***, Distributions of sIPSC amplitude for mutant neurons (*Mecp2*$^{F/y}$; *Emx1*-Cre, gray) and control neurons (*Mecp2*$^{wt/y}$; *Emx1*-Cre, black). The peak amplitude of sIPSCs for control (37.8 $\pm$ 2.3 pA) and mutant neurons (34.3 $\pm$ 1.5 pA; $p = 0.13$). ***D***, Averaged sIPSCs for control and mutant neurons. The mean decay constant of sIPSCs was 5.6 $\pm$ 0.2 ms for control neurons, and 4.9 $\pm$ 0.1 ms for mutant neurons ($p = 0.04$).

To elucidate the mechanisms underlying the shift in E/I balance in MeCP2-deficient brains, we examined the effect of *Mecp2* deletion on synaptic transmission in the mPFC, a region that plays an important role in cognitive functions, anxiety and social behaviors (Holmes and Wellman, 2009; Etkin et al., 2011; Yizhar et al., 2011). We performed whole-cell patch-clamp recording in acute brain slices from *Emx1-Mecp2* mutant mice (*Mecp2*$^{F/y}$; *Emx1*-Cre) and two littermate control groups (*Mecp2*$^{wt/y}$; *Emx1*-Cre and *Mecp2*$^{F/y}$) at P17–P20. We first assessed inhibitory synaptic transmission by recording spontaneous IPSCs (sIPSCs) from layer 5 pyramidal neurons in the mPFC. Excitatory synaptic transmission was blocked by DNQX (10 μM) and kynurenic acid (1 mM). *Emx1-Mecp2* mutant neurons showed fewer sIPSCs than control neurons at P17–P20 (Fig. 2*A*,*B*,*C*), whereas no difference was found between mutant and control neurons in the mean peak amplitude or kinetics of sIPSCs (Fig. 2*D*). Because sIPSCs may contain both quantal IPSCs (mIPSCs) and spontaneous spike-driven IPSCs, we selectively recorded mIPSCs in the presence of tetrodotoxin (0.5 μM). Mutant (*Mecp2*$^{F/y}$; *Emx1*-Cre) neurons showed fewer quantal events than control (*Mecp2*$^{wt/y}$; *Emx1*-Cre) neurons at P17–P20 (Fig. 2*E*). In mutant neurons the mean frequency of mIPSCs was reduced by 30%, without any change in the amplitude or kinetics of mIPSCs (Fig. 2*F*,*G*).

To determine whether GABAergic defects are present in young adult mutant mice, we recorded from layer 5 pyramidal neurons in mPFC of mice aged 6–7 weeks. The frequency of mIPSCs was significantly reduced in *Emx1-Mecp2* mutant neurons (5.8 $\pm$ 0.4 Hz, $n = 15$ cells from 3 mutant mice vs 7.3 $\pm$ 0.4 Hz, $n = 17$ cells from 3 control mice; $p = 0.008$), whereas the peak amplitude of mIPSCs was not different between mutant and control neurons (30.9 $\pm$ 1.6 pA for mutant vs 31.4 $\pm$ 2.0 pA for control; $p = 0.88$). These results are consistent with those obtained at 3 weeks of age, suggesting that deletion of *Mecp2* from excitatory neurons in the forebrain causes a significant reduction of GABAergic transmission in young adult mice.

To examine whether deletion of *Mecp2* alters excitatory transmission, we recorded mEPSCs from layer 5 pyramidal neurons in the mPFC of *Emx1-Mecp2* mutant and control mice at P17–P18 and 6–7 weeks of age. At P17–P18, there was no difference between mutant and control neurons in the frequency, amplitude, or decay time of mEPSCs (Fig. 3). Similar results were obtained at 6–7 weeks of age. At 6–7 weeks of age, the mean frequency of mEPSCs was 4.8 $\pm$ 0.8 Hz ($n = 15$ from 3 mice) for control neurons, and 5.8 $\pm$ 0.7 Hz ($n = 14$ from 3 mice) for mutant neurons ($p = 0.25$); the mean peak amplitude of mEPSCs was 14.2 $\pm$ 1.1 pA for control neurons, 12.9 $\pm$ 0.8 for mutant neurons ($p = 0.51$); decay constant of mEPSC was 4.2 $\pm$ 0.2 ms for control neurons, and 4.1 $\pm$ 0.1 ms for mutant neurons ($p = 0.39$). These results indicate a selective reduction of inhibitory synaptic transmission in mPFC of *Emx1-Mecp2* mice.

Although the mPFC is critically implicated in cognitive functions, its role in absence seizures is unclear. Previous studies have shown that in a rat model of absence seizure spike-wave discharges are initiated in the deep layers of the somatosensory cortex (Polack et al., 2007). Therefore we recorded from layer 5 pyramidal neurons in the somatosensory cortex (S1; Fig. 4). Similar to what we found in the mPFC, the frequency of sIPSCs was reduced by 25% in S1 neurons of *Emx1-Mecp2* mutant mice (Fig. 4*B*), without significant changes in the amplitude or decay time of sIPSCs (Fig. 4*C*,*D*). Similar results were obtained for mIPSCs. The mean frequency of mIPSCs was 7.1 $\pm$ 0.3 Hz ($n = 18$ cells from 3 mice) for mutant and 9.7 $\pm$ 0.4 Hz ($n = 23$ from 3 mice) for control ($p = 0.0001$); the mean peak amplitude of mIPSCs was 31.5 $\pm$ 1.4 pA for mutant and 35.3 $\pm$ 1.7 pA for control ($p = 0.124$); the decay constant was 5.4 $\pm$ 0.1 ms for mutant and 5.6 $\pm$ 0.1 ms for control ($p = 0.854$). We also recorded mEPSCs from layer 5 pyramidal neurons in S1 of mutant and control mice.

There was no significant difference between mutant and control neurons in the frequency (6.2 ± 0.6 Hz, $n = 16$ for mutant vs 5.6 ± 0.4 Hz, $n = 18$ for control; $p = 0.40$), amplitude (15.5 ± 0.3 pA for mutant vs 14.6 ± 0.4 pA for control; $p = 0.18$), or decay time (3.0 ± 0.1 ms for mutant vs 3.2 ± 0.1 ms for control; $p = 0.06$) of mEPSCs. Together, these results suggest that deletion of *Mecp2* from the cortical neurons selectively reduces GABAergic transmission in the cortex.

Deletion of *Mecp2* from forebrain inhibitory neurons has no effects on GABAergic transmission in layer 5 pyramidal neurons

Recent studies have shown that deletion of *Mecp2* from all inhibitory neurons in the brain reduces GABAergic transmission in the cortex (Chao et al., 2010). To determine whether MeCP2 in cortical inhibitory neurons plays a role in GABAergic transmission in the cortex, we examined GABAergic transmission in the cortex of conditional *Dlx6a-Mecp2* mice. In the *Dlx6a*-Cre strain, Cre recombinase is selectively expressed in GABAergic neurons in the forebrain (Monory et al., 2006). To ascertain the efficiency of deletion, we first performed GABA immunostaining on brain sections from mice that carried the *Dlx6a*-Cre and Rosa-tdTomato reporter. All GABA-positive neurons in the mPFC also expressed tdTomato (Fig. 4*A*), indicating that all GABAergic neurons in the mPFC of the *Dlx6a*-Cre mice express Cre recombinase. Approximately 10% of tdTomato-expressing cells in the mPFC of *Dlx6a*-Cre; Ai14 mice at P17–P18 did not show GABA immunoreactivity. These cells were smaller than GABA-positive ones, and presumably were immature interneurons. Next, we performed MeCP2 immunostaining on sections from conditional *Dlx6a-Mecp2* mutant mice (*Mecp2*$^{F/y}$;*Dlx6a*-Cre) carrying the Rosa-tdTomato reporter. All tdTomato-expressing cells were MeCP2-negative, whereas neighboring tdTomato-negative cells showed normal MeCP2 immunoreactivity (Fig. 5*B*). These results indicate that in *Dlx6a-Mecp2* mutant mice, *Mecp2* was deleted from all GABAergic neurons in the mPFC. Spontaneous GABAergic transmission was analyzed in layer 5 pyramidal neurons from *Dlx6a-Mecp2* mutant and control littermates at P17–P20. We found no difference between mutant and control neurons in the frequency, amplitude, or decay time of sIPSCs (Fig. 5*C–E*).

Similar results were obtained from layer 5 pyramidal neurons in the somatosensory cortex at P18–P20. The mean frequency of sIPSCs was 8.5 ± 0.3 Hz ($n = 17$ cells from 3 mice) for mutant, and 8.2 ± 0.4 Hz ($n = 20$ cells from 3 mice) for control ($p = 0.65$); the mean peak amplitude was 38.9 ± 2.7 pA for mutant, and 40.2 ± 2.1 pA for control ($p = 0.46$); the mean decay time was 5.5 ± 0.2 ms for mutant, and 5.1 ± 0.3 ms for control ($p = 0.43$). Together, these findings suggest that MeCP2 expression by cortical interneurons is not essential for the formation and function of GABAergic synapses in layer 5 pyramidal neurons.

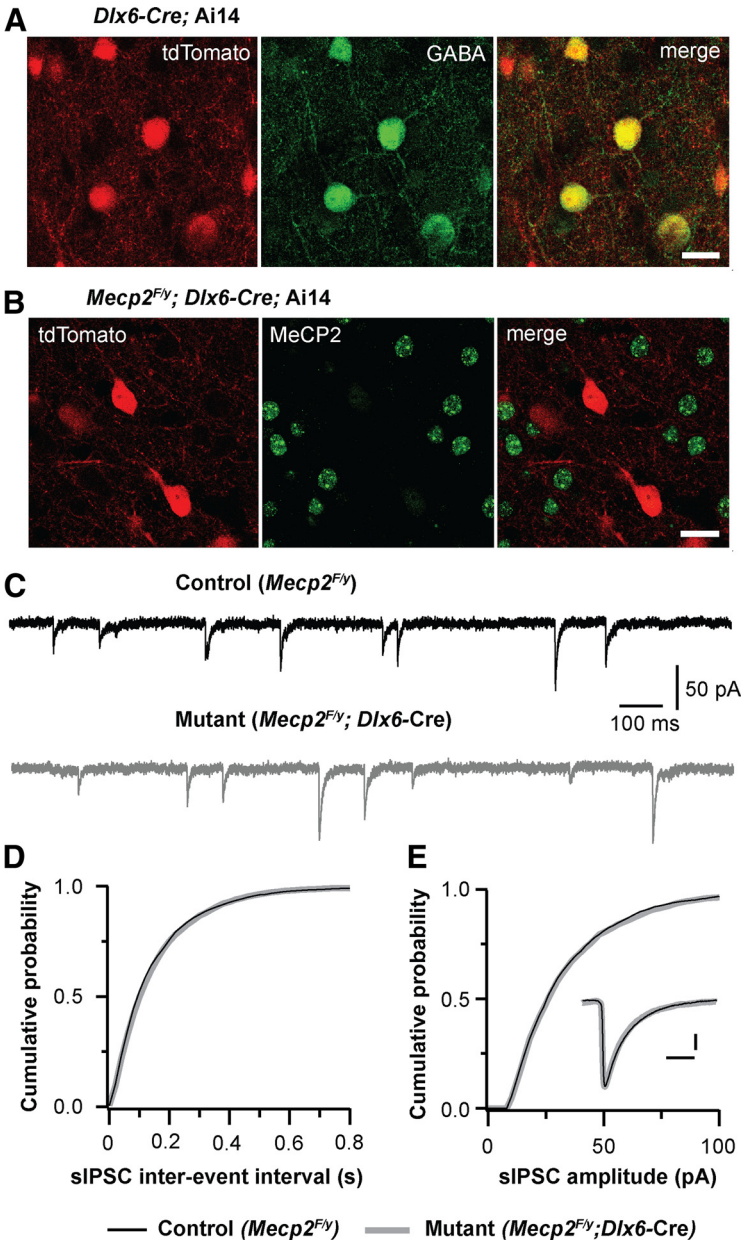

Figure 5. Selective deletion of *Mecp2* from forebrain GABAergic neurons had no effect on spontaneous GABAergic transmission. ***A***, tdTomato signal and GABA immunostaining in the mPFC of a *Dlx6a*-Cre; Ai14 mouse. Scale bar, 20 μm. ***B***, tdTomato signal and MeCP2 immunostaining in the mPFC of a *Mecp2*$^{F/y}$; *Dlx6a*-Cre; Ai14 mouse. Scale bar, 20 μm. ***C***, sIPSCs recorded from a control (*Mecp2*$^{F/y}$) and mutant (*Mecp2*$^{F/y}$; *Dlx6a*-Cre) neurons at P18. ***D***, Distributions of sIPSC intervals for control (black) and mutant (gray) neurons. The mean frequency of sIPSCs was 6.3 ± 0.4 Hz ($n = 15$ from 3 mice) for control neurons, and 6.0 ± 0.3 Hz ($n = 19$ from 3 mice) for mutant neurons ($p = 0.82$). ***E***, Distributions of sIPSC amplitude for control and mutant neurons. Inset, Averaged sIPSCs from control and mutant neurons. Scale bars, 10 ms and 10 pA. The mean amplitude of sIPSCs was 38.1 ± 3.0 pA for control neurons, and 36.9 ± 1.9 pA for mutant neurons ($p = 0.8$). The mean decay constant was 6.2 ± 0.3 ms for control neurons, and 5.7 ± 0.2 ms for mutant neurons ($p = 0.2$).

Defect of GABAergic transmission is restricted to neurons lacking MeCP2

In *Emx1-Mecp2* mutant mice, *Mecp2* was deleted from all neurons in the cortex. This large-scale removal of MeCP2 in the cortex may have indirect effects on GABAergic transmission. For example, *Mecp2* deletion may alter cortical activity, which in turn

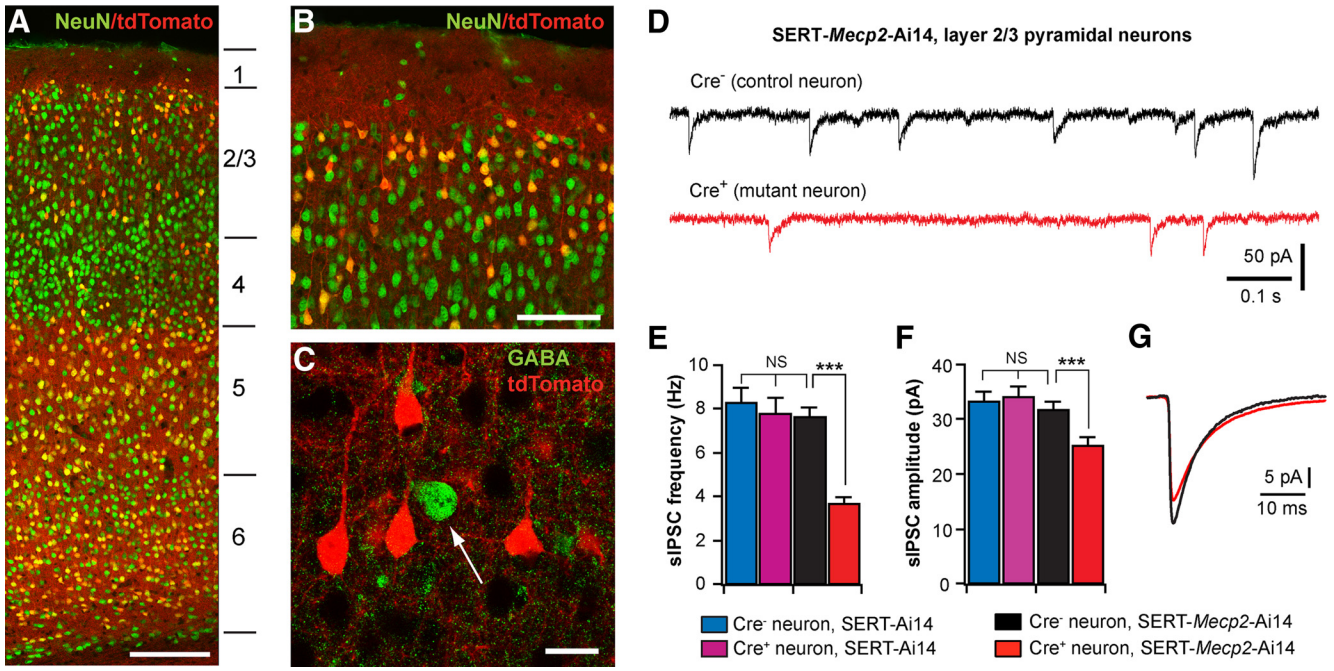

Figure 6. Mosaic deletion of *Mecp2* in the cortex selectively disrupts GABAergic transmission in neurons deficient in MeCP2. ***A***, confocal image of the S1 in coronal section of a SERT-Ai14 mouse at P21. Neurons were labeled with anti-NeuN (green); Cre^+ cells were identified with tdTomato signal (red). The lines and numbers on the side indicate the locations of the six cortical layers. Scale bar, 200 μm. ***B***, Layer 1 and upper layer 2/3 of S1 at a higher-magnification. Scale bar, 100 μm. Approximately 19% of neurons in upper layer 2/3 were Cre^+. ***C***, Layer 2/3 of S1 immunostained for GABA (green). The vast majority of Cre^+ neurons (red) in layer 2/3 were pyramidal neurons and negative for GABA. Scale bar, 20 μm. ***D***, sIPSCs recorded from a Cre^- (top trace, black) and a Cre^+ (bottom trace, red) pyramidal neurons in S1 layer 2/3 of a SERT-*Mecp2*-Ai14 mutant mouse at P18. ***E***, Mean frequency of sIPSCs from Cre^- and Cre^+ layer 2/3 pyramidal neurons in SERT-*Mecp2*-Ai14 mutant and SERT-Ai14 control mice at P17–P18. For mutant mice, the mean frequency was 7.6 ± 0.4 Hz ($n = 18$, for Cre^- neurons, black) and 3.6 ± 0.3 Hz ($n = 17$, for Cre^+ neurons, red; $^{***}p < 0.0005$). For control mice, the mean frequency was 8.3 ± 0.7 Hz ($n = 17$, for Cre^- neurons, blue) and 7.8 ± 0.7 Hz ($n = 17$, for Cre^+ neurons, purple). ***F***, Mean peak amplitude of sIPSCs for the four groups. The mean peak amplitude was 31.6 ± 1.6 pA (Cre^- neurons in mutant mice), 25.0 ± 1.6 pA (Cre^+ neurons in mutant mice), 33.3 ± 1.8 pA (Cre^- neurons in control mice), and 34.1 ± 1.9 pA (Cre^+ neurons in control mice); $^{***}p < 0.001$. ***G***, Averaged sIPSCs for Cre^- (in black) and Cre^+ (in red) neurons in mutant mice. The decay time constant of sIPSCs was 7.5 ± 0.2 ms (Cre^- neurons in mutant mice), 8.4 ± 0.2 ms (Cre^+ neurons in mutant mice), 7.4 ± 0.1 ms (Cre^- neurons in control mice), and 7.6 ± 0.2 ms (Cre^+ neurons in control mice). The decay time of Cre^+ neurons in mutant mice was significantly slower than the other three groups ($^{**}p = 0.002$).

leads to widespread changes in GABAergic transmission. In addition, Cre recombinase is also expressed in glia cells in the cortex of *Emx1*-Cre mice (Gorski et al., 2002), and deletion of *Mecp2* from glia cells may contribute to GABAergic defects. To examine these possibilities, we took advantage of the sparse expression of Cre recombinase in layer 2/3 of S1 of SERT-Cre mice. Using the Ai14 reporter (Madisen et al., 2010) and NeuN staining, we found that 19% (258 of 1339) of neurons in upper layer 2/3 of S1 in SERT-Cre mice were Cre^+ (Fig. 6*A*,*B*). Consistent with our previous results (Zhang et al., 2013), all Cre^+ cells in the cortex of SERT-cre mice were $NeuN^+$, indicating that Cre expression in these mice was restricted to neurons. Immunostaining for GABA indicated that 94% of Cre^+ neurons in layer 2/3 were pyramidal neurons and negative for GABA (Fig. 6C); in contrast, only 16% of GABA-positive neurons were Cre^+. We recorded from layer 2/3 pyramidal neurons in S1 of SERT-*Mecp2* mutant mice carrying the Ai14 reporter (SERT-*Mecp2*-Ai14, or $Mecp2^{F/y}$; SERT-Cre; Ai14). Cre^+ and Cre^- neurons were identified by epifluorescence of tdTomato. GABAergic transmission was significantly reduced in Cre^+ layer 2/3 pyramidal neurons compared with Cre^- ones in the same animals (Fig. 6*D*–*G*). The frequency of sIPSCs was reduced by 57% in mutant neurons (Fig. 6*E*, red and black bars), with a small reduction (20%) in sIPSC amplitude (Fig. 6*F*, red and black bars). To examine any side effects of Cre and tdTomato expression, we also recorded from Cre^+ and Cre^- neurons in SERT-Ai14 mice wild-type for *Mecp2* ($Mecp2^{wt/y}$; SERT-Cre; Ai14); there was no difference in sIPSCs between Cre^+ and Cre^- neurons of control mice (Fig. 6*E*,*F*, blue and purple bars). Together, these results demonstrate that the lack of MeCP2 in postsynaptic neurons causes a reduction of GABAergic transmission.

Forebrain-restricted deletion of *Mecp2* reduces the number of GABAergic synapses in the cortex

We further examined synaptic mechanisms by which MeCP2 regulates GABAergic transmission. The lack of change in the amplitude or kinetics of sIPSCs in *Emx1-Mecp2* mutant neurons indicates that alterations in presynaptic function or synapse number are the possible causes. We recorded evoked IPSCs in neurons from *Emx1-Mecp2* mutant and littermate control mice at P18–P20. Stimulation electrodes made of twisted microwires were placed 200 μm away from the recorded cell, and current pulses were applied at 1/15 s. Monosynaptic IPSCs were recorded from mutant and control neurons in the presence of DNQX and kynurenic acid (Fig. 7*A*). For each cell, the input–output relationship was determined by stimuli at a range of intensity. Mutant neurons showed similar IPSC threshold as control ones (Fig. 7*B*). However, peak amplitudes of IPSCs were significantly smaller in mutant neurons than control ones (Fig. 7*B*). The maximal IPSC, reached at about the same stimulus intensities in mutant and control neurons, was 2.6 ± 0.2 nA ($n = 14$) for mutant neurons, and 3.5 ± 0.3 nA ($n = 13$) for control neurons ($p = 0.02$). We recorded paired pulse responses at intensities that produced half-maximal IPSCs. There was no difference between mutant and control neurons in paired pulse ratio (Fig. 7*C*). These results indicate that a decrease in the number of GABAergic syn-

apses may be the primary cause of the reduction of GABAergic transmission in mutant neurons.

To analyze changes in the number of GABAergic synapses, we performed immunofluorescence staining of VGAT on brain sections from *Emx1-Mecp2* mutant and littermate control mice. At P18–P19, *Emx1-Mecp2* mutant mice showed significantly fewer VGAT-positive puncta in layer 5 of mPFC than control mice (Fig. 7*D*, top). The density of VGAT-positive puncta was reduced by 42% in layer 5 of mutant mice (Fig. 7*E*). Similar reductions (37%) were observed in young adult mutant mice at 7–8 weeks of age (Fig. 7*D*, bottom, *E*). These results indicate that conditional deletion of *Mecp2* with *Emx1*-Cre leads to reductions in the number of GABAergic synapses in the mPFC.

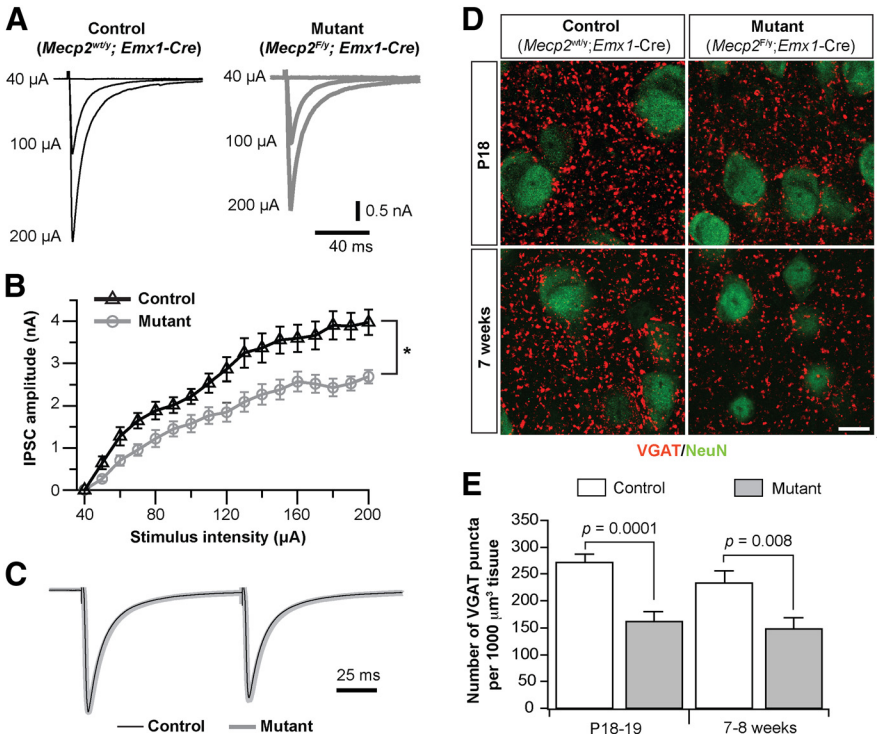

Figure 7. Evoked GABAergic transmission and the number of GABAergic synapses were reduced in the mPFC of *Emx1-Mecp2* mutant mice. ***A***, Monosynaptic IPSCs recorded from control and mutant neurons evoked by local stimulation. ***B***, The input–output curve of IPSCs for control ($n = 13$ from 3 mice) and mutant ($n = 14$ from 3 mice) neurons. ***C***, Paired pulse responses for IPSCs from control and mutant neurons. The averaged IPSCs from control and mutant neurons were normalized to the peak of the first IPSC. The paired pulse ratio at 100 ms interval was 0.89 ± 0.02 ($n = 10$ from 3 mice) for mutant neurons, and 0.85 ± 0.03 ($n = 11$ from 3 mice) for control neurons ($p = 0.14$). ***D***, Double immunostaining of VGAT (red) and NeuN (green) in the mPFC of control and mutant mice at P18 (top) and 7 weeks of age (bottom). Scale bar, 10 μm. ***E***, Numbers of VGAT puncta per 1000 μm^3 volume in layer 5 of mPFC of mutant and control mice at P18–P19 and 7–8 weeks of age. Data were obtained from four pairs of mice at P18–P19 and 7–8 weeks of age, respectively; three measurements were performed for each mouse. *P* values were obtained with Mann–Whitney test.

Deletion of *Mecp2* enhances neuronal discharges through disinhibition

Our results so far suggest that selective deletion of *Mecp2* from cortical neurons reduces GABAergic transmission. To determine the effect of *Mecp2* deletion on neuronal activity, we performed current-clamp recordings from layer 5 pyramidal neurons of the mPFC in slices obtained from *Emx1-Mecp2* mutant mice and control littermates at P18–P20. Neuronal firing was examined first at the resting potential (typically ~−59 mV), and then at −53 mV by applying a small depolarizing current to adjust the interspike membrane potential. At the resting potential, neither mutant nor control neurons showed any spontaneous firing (Fig. 8*A*). At −53 mV, more mutant neurons (24/26) fired action potential than control (15/22; $p = 0.033$, Fisher's exact test). The average firing rate was significantly higher in mutant neurons (Fig. 8*B*).

The increased firing observed in mutant neurons could be due to changes in either intrinsic excitability of neurons or synaptic activity; these two possibilities are not mutually exclusive. Our results on synaptic activity suggest that a reduction of GABAergic transmission contributes to the hyperexcitation of *Mecp2* mutant neurons. We reasoned that if a reduction in GABAergic transmission is the cause of hyperexcitation in mutant neurons, blocking GABAergic transmission in both control and mutant neurons should abolish the difference between them. Because bath application of $GABA_A$ antagonists causes epileptiform activity in cortical slices, we used intracellular application of picrotoxin to block GABAergic transmission in single cells (Inomata et al., 1988). Picrotoxin (0.5 mM) included in the patch pipette blocked sIPSCs in pyramidal neurons (Fig. 8*C*). Picrotoxin abolished the difference between *Emx1-Mecp2* mutant and control neurons in firing, and enhanced firing in both mutant and control neurons (Fig. 8*D*,*E*). These results suggest that conditional deletion of *Mecp2* with *Emx1*-Cre causes hyperexcitation of layer 5 pyramidal neurons by reducing GABAergic transmission in the cortex.

We next assessed intrinsic excitability of layer 5 pyramidal neurons in the mPFC in the presence of synaptic blockers picrotoxin (100 μM), DNQX (10 μM), and kynurenic acid (1 mM). Firing was evoked by a series of depolarizing current steps (Fig. 8*F*). The curve of the mean firing rate vs injected current was not different between mutant and control neurons (Fig. 8*G*). Furthermore, there was no difference between mutant and control neurons in resting potential (-60.8 ± 0.4 mV, $n = 27$, for control; -59.9 ± 0.4 mV, $n = 31$ for mutant; $p = 0.08$), input resistance (125 ± 8 MΩ for control; 113 ± 7 MΩ for mutant; $p = 0.19$), or spike threshold (-38.1 ± 0.4 mV for control; -38.6 ± 0.5 mV for mutant; $p = 0.41$). These results indicate that intrinsic excitability of layer 5 pyramidal neurons was not altered by *Mecp2* deletion.

Discussion

Our results suggest that MeCP2 in cortical excitatory neurons has a key role in regulating GABAergic transmission and excitability of cortical circuits. Deletion of *Mecp2* from excitatory but not inhibitory neurons in the forebrain leads to seizures, hyperexcitation, and a reduction of GABAergic transmission. Using pharmacological manipulation at the single-cell level, we provide evidence that loss of MeCP2 from cortical neurons leads to enhanced excitability through a reduction of GABAergic transmission.

Seizure and cortical excitability in MeCP2-deficient brain

Studies from several patient groups have shown that seizure is a common feature of RTT (Jian et al., 2007; Nissenkorn et al., 2010; Pintaudi et al., 2010; Cardoza et al., 2011). Both partial and generalized seizures are common among RTT patients (Cardoza et al., 2011). The types of generalized seizures at the onset showed a

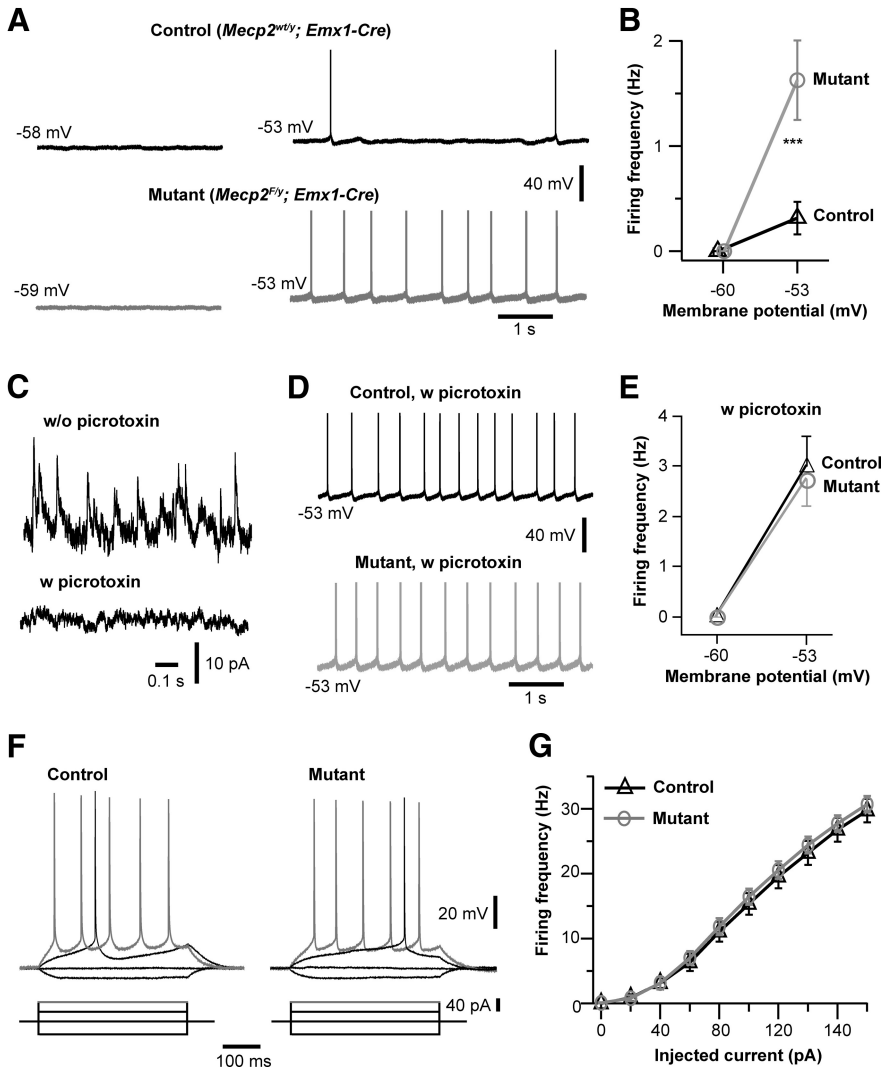

Figure 8. Hyperexcitation of cortical neurons in *Emx1-Mecp2* mutant mice. ***A***, Neuronal activity at the resting potential (−58, −59 mV) and at −53 mV in a control (*Mecp2*$^{wt/y}$; *Emx1*-Cre) and mutant (*Mecp2*$^{F/y}$; *Emx1*-Cre) neurons. ***B***, Frequency of action potential of control and mutant neurons at the resting potential and at −53 mV. The mean firing frequency at −53 mV was 0.3 ± 0.2 Hz for control ($n = 21$ from 3 mice), and 1.6 ± 0.4 Hz for mutant ($n = 26$ from 3 mice; ***$p < 0.001$). ***C***, Spontaneous IPSCs recorded from wild-type neurons without and with picrotoxin (0.5 mM) in the patch pipette. These recordings were obtained at 0 mV with the pipette solution containing Cs-methylsulfate ($[Cl^-]_i$ of 35 mM). ***D***, Firing recorded from a control and mutant neurons at −53 mV with picrotoxin in the patch pipettes. ***E***, Firing frequency of control and mutant neurons at −60 and −53 mV with intracellular picrotoxin. The mean firing frequency at −53 mV was 3.0 ± 0.6 Hz for control ($n = 24$ from 3 mice), and 2.7 ± 0.5 Hz for mutant ($n = 23$ from 3 mice; $p = 0.86$). ***F***, Membrane potential changes in response to current steps in control and mutant neurons. Synaptic transmission was blocked by bath perfusion of DNQX, kynurenic acid, and picrotoxin. ***G***, Plot of spike frequency versus injected current for control ($n = 27$ from 3 mice) and mutant neurons ($n = 31$ from 3 mice).

wide spectrum; the largest group had generalized tonic-clonic seizures, and this is followed by the group showing atypical absence seizures (Pintaudi et al., 2010). Mouse models of RTT recapitulate the seizure phenotype. Recurrent seizures were found in both male (*Mecp2*$^{-/y}$) and female heterozygote animals (Shahbazian et al., 2002; Chao et al., 2010; D'Cruz et al., 2010). In female *Mecp2* heterozygote mice, spike-wave discharges of 1–2 s in duration were detected in the cortex (D'Cruz et al., 2010). These spontaneous discharges occurred in wake immobile mice, and were sensitive to ethosuximide. Overall, EEG results obtained from RTT patients and *Mecp2* mutant mice indicate a hyperexcitation of the cortex and associated regions in MeCP2-deficient brains.

In contrast to *in vivo* data, early studies using brain slices showed a reduction of firing in cortical pyramidal neurons of germline *Mecp2* knock-out mice, and the effect was associated with a reduction of excitatory transmission (Dani et al., 2005). In the present study, we obtained different results: cortical pyramidal neurons in *Emx1-Mecp2* mice showed an increase of firing and the effect was associated with a reduction of inhibitory transmission without any change in quantal excitatory transmission. The reason for this discrepancy is unknown. One possibility is the differences in experimental methods. The previous study used low concentrations of divalent cations (0.5 mM Mg^{2+} and 1.0 mM Ca^{2+}) for the recording of cell firing and synaptic currents (Dani et al., 2005), whereas we used physiological concentrations of divalent cations (1.3 mM Mg^{2+} and 1.5 mM Ca^{2+}). Neurons and synapses in MeCP2-deficient brains may be different from wild-type neurons in response to low concentrations of Mg^{2+} and Ca^{2+}. Although no change in intrinsic excitability was found in the previous study, those experiments were conducted in ACSF containing higher concentrations of divalent cations (2 mM Mg^{2+} and 2 mM Ca^{2+}). It is also unclear whether the reduction in excitatory transmission observed in the previous study significantly contributed to the change in cell firing. There was a 15% reduction in mEPSC amplitude without significant change in mEPSC frequency, and no significant change in the amplitude or frequency of mIPSCs was observed (Dani et al., 2005). In hippocampal neurons, deletion of *Mecp2* reduced the frequency but not amplitude of mEPSCs, and the effect was associated with a reduction of the number of glutamatergic synapses (Chao et al., 2007). However, the difference in the number of glutamatergic synapses was observed at 2 weeks of age, but not at 5 weeks of age. It should be noted that our analysis of excitatory transmission was limited to mEPSCs. Therefore, we cannot exclude the possibility that MeCP2 may regulate some aspects of presynaptic function at cortical excitatory synapses. A recent study has shown reductions of visual acuity and neuronal activity in visual cortical neurons of adult *Mecp2* knock-out mice (Durand et al., 2012). These effects appeared to be restricted to layer 4 neurons in the visual cortex, and may be related to defects of synaptic transmission observed at retinogeniculate synapses in *Mecp2* knock-out mice (Noutel et al., 2011).

Another possibility is the difference in genetic background. Although the previous study used mice on a mixed 129/B6/BALB background (Dani et al., 2005), our studies were conducted in mice on a predominantly B6 background. Because of the complex role of MeCP2 in transcriptional regulation (Chahrour et al., 2008; Guy et al., 2011), genetic background may have a strong

effect on disease phenotypes. Indeed results from a recent study using female *Mecp2* heterozygous mutant mice indicate that genetic background has significant effects on behavioral phenotypes including anxiety-like behavior and prepulse inhibition (Samaco et al., 2013). Previous studies have reported that MeCP2-deficient mice on a B6 background exhibit hyperexcitability discharges and seizures (Chao et al., 2010; D'Cruz et al., 2010). Our results are consistent with these findings.

GABAergic dysfunction in MeCP2-deficient brain

Several studies reported reductions of GABAergic transmission in MeCP2-deficient brain. In both the brainstem and thalamus of *Mecp2* knock-out mice, the reduction of GABAergic transmission was associated with a decrease in the number of GABAergic synapses (Medrihan et al., 2008; Zhang et al., 2010). Our results indicate that similar changes occur in the cortex. *Emx1-Mecp2* mutant mice showed reductions in mIPSC frequency and the number of VGAT-positive puncta in the cortex. There was little change in the amplitude or kinetics of mIPSC, and the reduction in mIPSC frequency was comparable to the change in the number of GABAergic synaptic terminals. These results suggest that a major consequence of *Mecp2* deletion is a downregulation of GABAergic innervation.

A recent study showed that deletion of *Mecp2* from all GABAergic neurons in the brain using a *Viaat*-Cre driver led to cortical hyperexcitation, but selective deletion of *Mecp2* from forebrain GABAergic neurons using *Dlx5/6*-Cre did not cause hyperexcitation (Chao et al., 2010). This latter observation is confirmed by our results using the same Cre driver with a different nomenclature *Dlx6a*-Cre. *Dlx6a-Mecp2* mutant mice did not show any spike-wave discharges, and our immunostaining data demonstrated that *Mecp2* was deleted from all cortical GABAergic neurons in *Dlx6a-Mecp2* mice. Spontaneous GABAergic transmission was not altered in cortical neurons in *Dlx6a-Mecp2* mice. In contrast, *Viaat-Mecp2* mutant mice showed reductions of GAD and GABA levels in the cortex and striatum, and smaller mIPSCs (Chao et al., 2010). It is possible that loss of MeCP2 from hindbrain inhibitory neurons may have a broad impact on GABAergic function in the brain.

It remains unclear how the loss of MeCP2 causes dysfunction of GABAergic transmission. MeCP2 is expressed in all neuronal tissues by neurons, glia, and microglia (Ballas et al., 2009; Maezawa et al., 2009; Maezawa and Jin, 2010; Lioy et al., 2011). Although MeCP2 in glia has been implicated in changes in dendritic morphology and level of vesicular glutamate transporter in *Mecp2*-knock-out mice, the role of glial MeCP2 in GABAergic transmission is unknown. Our single-cell deletion analysis in SERT-*Mecp2* mutant mice suggests that glial MeCP2 is not essential for GABAergic defects in cortical pyramidal neurons in mutant mice. However, we cannot exclude the possibility that MeCP2 in glia is implicated in GABAergic transmission in other brain regions.

Deletion of *Mecp2* from all excitatory neurons in the cortex may alter GABAergic transmission through activity-dependent network effects. However, our results of single-cell deletion showed that the loss of MeCP2 from a small number of cortical pyramidal neurons caused a selective reduction of GABAergic transmission in these neurons. Our finding suggests a model where MeCP2 in postsynaptic neurons regulates retrograde signaling at GABAergic synapses. As a transcriptional regulator, MeCP2 has a large number of target genes (Chahrour et al., 2008), and therefore may regulate GABAergic innervation through multiple pathways. MeCP2 has been implicated in the regulation of brain-derived neurotrophic factor (BDNF; Wang et al., 2006; Zhou et al., 2006; Li et al., 2012); loss of BDNF from single neurons leads to a reduction of GABAergic innervation (Kohara et al., 2007); increasing BDNF level in the brain of *Mecp2* mutant mice rescues some neurological defects (Chang et al., 2006; Kline et al., 2010). However, the level of BDNF was not altered in the brain of *Mecp2* knock-out mice at 2 weeks of age, and was only slightly reduced in the cortex of mutant mice at 6–8 weeks of age (Chang et al., 2006). BDNF signaling was impaired in hippocampal pyramidal neurons in *Mecp2* knock-out mice (Li et al., 2012). Future studies are needed to determine whether MeCP2 regulates BDNF signaling in GABAergic neurons.

So far GABAergic defects have been reported in mice with either germline *Mecp2* deletion or conditional *Mecp2* deletion using early onset Cre drivers. In our case, both *Emx1*-Cre and SERT-Cre are expressed by birth in the cortex. Together with other studies in the brainstem and thalamus (Medrihan et al., 2008; Zhang et al., 2010), our results suggest that MeCP2 plays an important role in the maturation of GABAergic synapses in the developing brain. On the other hand, MeCP2 is required in the adult for normal brain function (Guy et al., 2007; McGraw et al., 2011; Cheval et al., 2012). It may be interesting and important to know whether MeCP2 plays a role in the maintenance and plasticity of GABAergic synapses in adult brain.

References

Armstrong DD (2005) Neuropathology of Rett syndrome. J Child Neurol 20:747–753. CrossRef Medline

Asaka Y, Jugloff DG, Zhang L, Eubanks JH, Fitzsimonds RM (2006) Hippocampal synaptic plasticity is impaired in the Mecp2-null mouse model of Rett syndrome. Neurobiol Dis 21:217–227. CrossRef Medline

Ballas N, Lioy DT, Grunseich C, Mandel G (2009) Non-cell autonomous influence of MeCP2-deficient glia on neuronal dendritic morphology. Nat Neurosci 12:311–317. CrossRef Medline

Beyer B, Deleuze C, Letts VA, Mahaffey CL, Boumil RM, Lew TA, Huguenard JR, Frankel WN (2008) Absence seizures in C3H/HeJ and knockout mice caused by mutation of the AMPA receptor subunit Gria4. Hum Mol Genet 17:1738–1749. CrossRef Medline

Calfa G, Hablitz JJ, Pozzo-Miller L (2011) Network hyperexcitability in hippocampal slices from Mecp2 mutant mice revealed by voltage-sensitive dye imaging. J Neurophysiol 105:1768–1784. CrossRef Medline

Cardoza B, Clarke A, Wilcox J, Gibbon F, Smith PE, Archer H, Hryniewiecka-Jaworska A, Kerr M (2011) Epilepsy in Rett syndrome: association between phenotype and genotype, and implications for practice. Seizure 20:646–649. CrossRef Medline

Chahrour M, Zoghbi HY (2007) The story of Rett syndrome: from clinic to neurobiology. Neuron 56:422–437. CrossRef Medline

Chahrour M, Jung SY, Shaw C, Zhou X, Wong ST, Qin J, Zoghbi HY (2008) MeCP2, a key contributor to neurological disease, activates and represses transcription. Science 320:1224–1229. CrossRef Medline

Chang Q, Khare G, Dani V, Nelson S, Jaenisch R (2006) The disease progression of Mecp2 mutant mice is affected by the level of BDNF expression. Neuron 49:341–348. CrossRef Medline

Chao HT, Zoghbi HY, Rosenmund C (2007) MeCP2 controls excitatory synaptic strength by regulating glutamate synapse number. Neuron 56:58–65. CrossRef Medline

Chao HT, Chen H, Samaco RC, Xue M, Chahrour M, Yoo J, Neul JL, Gong S, Lu HC, Heintz N, Ekker M, Rubenstein JL, Noebels JL, Rosenmund C, Zoghbi HY (2010) Dysfunction in GABA signalling mediates autism-like stereotypies and rett syndrome phenotypes. Nature 468:263–269. CrossRef Medline

Chen RZ, Akbarian S, Tudor M, Jaenisch R (2001) Deficiency of methyl-CpG binding protein-2 in CNS neurons results in a Rett-like phenotype in mice. Nat Genet 27:327–331. CrossRef Medline

Cheval H, Guy J, Merusi C, De Sousa D, Selfridge J, Bird A (2012) Postnatal inactivation reveals enhanced requirement for MeCP2 at distinct age windows. Hum Mol Genet 21:3806–3814. CrossRef Medline

Dani VS, Chang Q, Maffei A, Turrigiano GG, Jaenisch R, Nelson SB (2005) Reduced cortical activity due to a shift in the balance between excitation

and inhibition in a mouse model of Rett syndrome. Proc Natl Acad Sci U S A 102:12560–12565. CrossRef Medline

D'Cruz JA, Wu C, Zahid T, El-Hayek Y, Zhang L, Eubanks JH (2010) Alterations of cortical and hippocampal EEG activity in MeCP2-deficient mice. Neurobiol Dis 38:8–16. CrossRef Medline

Durand S, Patrizi A, Quast KB, Hachigian L, Pavlyuk R, Saxena A, Carninci P, Hensch TK, Fagiolini M (2012) NMDA receptor regulation prevents regression of visual cortical function in the absence of Mecp2. Neuron 76:1078–1090. CrossRef Medline

Etkin A, Egner T, Kalisch R (2011) Emotional processing in anterior cingulate and medial prefrontal cortex. Trends Cogn Sci 15:85–93. CrossRef Medline

Gong S, Doughty M, Harbaugh CR, Cummins A, Hatten ME, Heintz N, Gerfen CR (2007) Targeting Cre recombinase to specific neuron populations with bacterial artificial chromosome constructs. J Neurosci 27:9817–9823. CrossRef Medline

Gorski JA, Talley T, Qiu M, Puelles L, Rubenstein JL, Jones KR (2002) Cortical excitatory neurons and glia, but not GABAergic neurons, are produced in the Emx1-expressing lineage. J Neurosci 22:6309–6314. Medline

Guy J, Hendrich B, Holmes M, Martin JE, Bird A (2001) A mouse Mecp2-null mutation causes neurological symptoms that mimic Rett syndrome. Nat Genet 27:322–326. CrossRef Medline

Guy J, Gan J, Selfridge J, Cobb S, Bird A (2007) Reversal of neurological defects in a mouse model of Rett syndrome. Science 315:1143–1147. CrossRef Medline

Guy J, Cheval H, Selfridge J, Bird A (2011) The role of MeCP2 in the brain. Annu Rev Cell Dev Biol 27:631–652. CrossRef Medline

Holmes A, Wellman CL (2009) Stress-induced prefrontal reorganization and executive dysfunction in rodents. Neurosci Biobehav Rev 33:773–783. CrossRef Medline

Inomata N, Tokutomi N, Oyama Y, Akaike N (1988) Intracellular picrotoxin blocks pentobarbital-gated Cl^- conductance. Neurosci Res 6:72–75. CrossRef Medline

Jian L, Nagarajan L, de Klerk N, Ravine D, Christodoulou J, Leonard H (2007) Seizures in Rett syndrome: an overview from a one-year calendar study. Eur J Paediatr Neurol 11:310–317. CrossRef Medline

Kline DD, Ogier M, Kunze DL, Katz DM (2010) Exogenous brain-derived neurotrophic factor rescues synaptic dysfunction in Mecp2-null mice. J Neurosci 30:5303–5310. CrossRef Medline

Kohara K, Yasuda H, Huang Y, Adachi N, Sohya K, Tsumoto T (2007) A local reduction in cortical GABAergic synapses after a loss of endogenous brain-derived neurotrophic factor, as revealed by single-cell gene knockout method. J Neurosci 27:7234–7244. CrossRef Medline

Li W, Calfa G, Larimore J, Pozzo-Miller L (2012) Activity-dependent BDNF release and TRPC signaling is impaired in hippocampal neurons of Mecp2 mutant mice. Proc Natl Acad Sci U S A 109:17087–17092. CrossRef Medline

Lioy DT, Garg SK, Monaghan CE, Raber J, Foust KD, Kaspar BK, Hirrlinger PG, Kirchhoff F, Bissonnette JM, Ballas N, Mandel G (2011) A role for glia in the progression of Rett's syndrome. Nature 475:497–500. CrossRef Medline

Madisen L, Zwingman TA, Sunkin SM, Oh SW, Zariwala HA, Gu H, Ng LL, Palmiter RD, Hawrylycz MJ, Jones AR, Lein ES, Zeng H (2010) A robust and high-throughput Cre reporting and characterization system for the whole mouse brain. Nat Neurosci 13:133–140. CrossRef Medline

Maezawa I, Jin LW (2010) Rett syndrome microglia damage dendrites and synapses by the elevated release of glutamate. J Neurosci 30:5346–5356. CrossRef Medline

Maezawa I, Swanberg S, Harvey D, LaSalle JM, Jin LW (2009) Rett syndrome astrocytes are abnormal and spread MeCP2 deficiency through gap junctions. J Neurosci 29:5051–5061. CrossRef Medline

McGraw CM, Samaco RC, Zoghbi HY (2011) Adult neural function requires MeCP2. Science 333:186. CrossRef Medline

Medrihan L, Tantalaki E, Aramuni G, Sargsyan V, Dudanova I, Missler M, Zhang W (2008) Early defects of GABAergic synapses in the brain stem of a MeCP2 mouse model of Rett syndrome. J Neurophysiol 99:112–121. CrossRef Medline

Monory K, Massa F, Egertová M, Eder M, Blaudzun H, Westenbroek R, Kelsch W, Jacob W, Marsch R, Ekker M, Long J, Rubenstein JL, Goebbels S, Nave KA, During M, Klugmann M, Wölfel B, Dodt HU, Zieglgänsberger W, Wotjak CT, Mackie K, Elphick MR, et al. (2006) The endocannabinoid system controls key epileptogenic circuits in the hippocampus. Neuron 51:455–466. CrossRef Medline

Moretti P, Levenson JM, Battaglia F, Atkinson R, Teague R, Antalffy B, Armstrong D, Arancio O, Sweatt JD, Zoghbi HY (2006) Learning and memory and synaptic plasticity are impaired in a mouse model of Rett syndrome. J Neurosci 26:319–327. CrossRef Medline

Na ES, Nelson ED, Adachi M, Autry AE, Mahgoub MA, Kavalali ET, Monteggia LM (2012) A mouse model for MeCP2 duplication syndrome: MeCP2 overexpression impairs learning and memory and synaptic transmission. J Neurosci 32:3109–3117. CrossRef Medline

Nelson ED, Kavalali ET, Monteggia LM (2006) MeCP2-dependent transcriptional repression regulates excitatory neurotransmission. Curr Biol 16:710–716. CrossRef Medline

Nissenkorn A, Gak E, Vecsler M, Reznik H, Menascu S, Ben Zeev B (2010) Epilepsy in Rett syndrome: the experience of a national Rett center. Epilepsia 51:1252–1258. CrossRef Medline

Noutel J, Hong YK, Leu B, Kang E, Chen C (2011) Experience-dependent retinogeniculate synapse remodeling is abnormal in MeCP2-deficient mice. Neuron 70:35–42. CrossRef Medline

Pintaudi M, Calevo MG, Vignoli A, Parodi E, Aiello F, Baglietto MG, Hayek Y, Buoni S, Renieri A, Russo S, Cogliati F, Giordano L, Canevini M, Veneselli E (2010) Epilepsy in Rett syndrome: clinical and genetic features. Epilepsy Behav 19:296–300. CrossRef Medline

Polack PO, Guillemain I, Hu E, Deransart C, Depaulis A, Charpier S (2007) Deep layer somatosensory cortical neurons initiate spike-and-wave discharges in a genetic model of absence seizures. J Neurosci 27:6590–6599. CrossRef Medline

Samaco RC, McGraw CM, Ward CS, Sun Y, Neul JL, Zoghbi HY (2013) Female Mecp2(±) mice display robust behavioral deficits on two different genetic backgrounds providing a framework for pre-clinical studies. Hum Mol Genet 22:96–109. CrossRef Medline

Shahbazian M, Young J, Yuva-Paylor L, Spencer C, Antalffy B, Noebels J, Armstrong D, Paylor R, Zoghbi H (2002) Mice with truncated MeCP2 recapitulate many Rett syndrome features and display hyperacetylation of histone H3. Neuron 35:243–254. CrossRef Medline

Taneja P, Ogier M, Brooks-Harris G, Schmid DA, Katz DM, Nelson SB (2009) Pathophysiology of locus ceruleus neurons in a mouse model of Rett syndrome. J Neurosci 29:12187–12195. CrossRef Medline

Vignoli A, Fabio RA, La Briola F, Giannatiempo S, Antonietti A, Maggiolini S, Canevini MP (2010) Correlations between neurophysiological, behavioral, and cognitive function in Rett syndrome. Epilepsy Behav 17:489–496. CrossRef Medline

Wang H, Chan SA, Ogier M, Hellard D, Wang Q, Smith C, Katz DM (2006) Dysregulation of brain-derived neurotrophic factor expression and neurosecretory function in Mecp2 null mice. J Neurosci 26:10911–10915. CrossRef Medline

Yizhar O, Fenno LE, Prigge M, Schneider F, Davidson TJ, O'Shea DJ, Sohal VS, Goshen I, Finkelstein J, Paz JT, Stehfest K, Fudim R, Ramakrishnan C, Huguenard JR, Hegemann P, Deisseroth K (2011) Neocortical excitation/inhibition balance in information processing and social dysfunction. Nature 477:171–178. CrossRef Medline

Zhang L, He J, Jugloff DG, Eubanks JH (2008) The MeCP2-null mouse hippocampus displays altered basal inhibitory rhythms and is prone to hyperexcitability. Hippocampus 18:294–309. CrossRef Medline

Zhang ZW (2004) Maturation of layer V pyramidal neurons in the rat prefrontal cortex: intrinsic properties and synaptic function. J Neurophysiol 91:1171–1182. CrossRef Medline

Zhang ZW, Arsenault D (2005) Gain modulation by serotonin in pyramidal neurons of the rat prefrontal cortex. J Physiol 566:379–394. CrossRef Medline

Zhang ZW, Zak JD, Liu H (2010) MeCP2 is required for normal development of GABAergic circuits in the thalamus. J Neurophysiol 103:2470–2481. CrossRef Medline

Zhang ZW, Peterson M, Liu H (2013) Essential role of postsynaptic NMDA receptors in developmental refinement of excitatory synapses. Proc Natl Acad Sci U S A 110:1095–1100. CrossRef Medline

Zhou Z, Hong EJ, Cohen S, Zhao WN, Ho HY, Schmidt L, Chen WG, Lin Y, Savner E, Griffith EC, Hu L, Steen JA, Weitz CJ, Greenberg ME (2006) Brain-specific phosphorylation of MeCP2 regulates activity-dependent Bdnf transcription, dendritic growth, and spine maturation. Neuron 52:255–269. CrossRef Medline